Electronic transport in GAA silicon nanowire MOSFETs: from Kubo-Greenwood mobility including screening remote coulomb scattering to analytical backscattering coefficient

J. Dura[1,2], F. Triozon[1], D. Munteanu[2], S. Barraud[1], S. Martinie[1], J.L. Autran[2]

[1] CEA-LETI MINATEC, 17 rue des Martyrs, 38054 Grenoble, Cedex 9, France

[2] IM2NP-CNRS, UMR CNRS 6242, Bât. IRPHE, 49 rue Joliot Curie, BP 146, 13384 Marseille Cedex 13, France

(e-mail : julien.dura@im2np.fr, Phone: +33 4 38 78 65 32, Fax:+33 4 38 78 51 40)

ABSTRACT

This paper presents the study of electron mobility in intrinsic silicon nanowires using the Kubo-Greenwood approach. This architecture (now considered as a realistic technology [1,2]) is aimed for ultra-scaled devices up to technology nodes sub-11nm [3] with silicon films of some nanometers. At these dimensions, the transport regime is completely modified due to the multi-subband transport. However, the promising potentialities of nanowires for microelectronic applications are not still demonstrated at all simulation levels (from atomistic to circuit performances). That is why the electronic transport is here investigated numerically using the Kubo-Greenwood approach coupled to a self-consistent Schrödinger-Poisson solver. Then, to support compact modelling including ultimate physical phenomena, an analytical model of the electron mobility and backscattering coefficient is exposed. The geometry dependence is essentially pointed out on the backscattering coefficient for a wide range of channel lengths (up to 10nm) and diameters (3nm $\leq\varnothing\leq$20nm).

KUBO-GRENNWOOD INVESTIGATION FOR ELECTRON MOBILITY

The mobility is computed in intrinsic cylindrical nanowires using the Kubo-Greenwood formula [4,5] based on the relaxation time approximation. Main scattering mechanisms pointed out by experimental investigations are considered: phonons *ph*, surface roughness *SR* and remote coulomb scattering *RCS*. Each interaction frequency is estimated using the Fermi golden rule based on the effective mass approximations. Phonon and surface roughness scattering mechanism are given in accordance with the literature [6-8]. The last mechanism, *RCS*, due to trapped charges in the high-k/metal gate stack is investigated by solving the Poisson equation considering a local charge in the oxide. Then, screening effect due to the accumulated charge in the silicon film is considered and an expression is proposed as a correction of the potential. The result is that screening effect is not negligible as we can see figure 1 on the RCS interaction frequency of the first tranverse subband. Finally, the total mobility including all scattering mechanisms is exposed and an analytical model reproducing the diameter dependence is developed (Eq.1) inspired from the theory. Figure 2 shows the comparison between the analytical model and numerical results for the low-field electron mobility for the different scattering mechanisms as a function of the diameter (a), (b) and (c). Then, the total mobility is plotted with respect to the electron density (d). We can note that the mobility is strongly impacted by the geometry for nanowire diameter less than 10nm.

BACKSCATTERING COEFFICIENT

The backscattering coefficient is the basis of the flux method initiated by McKelvey [9] and then developed by Natori/Lundstrom [10,11]. It defines the probability of carriers to be reflected back in the channel length and so the quality of the transport regime of the device as illustrated in figure 3. In equation 2, the backscattering coefficient R is described with a unified model valid for low and high electric field [9,13]. Two main concepts can be pointed out: the dynamical mean free path *dfp* which is directly related to the mobility and the “kT-layer” which represents the impact of interactions on the energy barrier of the transistor. The “kT-layer” length [11] is modeled and validated on numerical simulations as shown in our previous work [14]. Then, R is computed introducing the analytical model of the mobility calibrated on Kubo-Greenwood results. Figure 4 plots the analytical backscattering coefficient versus the channel length for different diameters at low (charge equal to $10^{11}cm^{-2}$) and high (charge equal to $10^{13}cm^{-2}$) inversion regime. By reducing the channel length, we can note that the transport in the nanowire is improved toward a theoretical ballistic regime (R=0). However, reducing the diameter tends to limit the mobility (as we saw for Kubo-Greenwood results) and, as a consequence, the backscattering of carriers in the channel is higher. For high charge, the impact of the diameter seems to be attenuated. In the full paper version, results concerning the backscattering coefficient will be validated on numerical simulations using a deterministic Wigner solver [15].

REFERENCES

[1] K.H. Cho *et al*, *IEEE Elect. Devices Lett*., vol. 28, no. 12, pp. 1129-1131, 2007.
[2] K. Tachi *et al*, *IEDM Tech. Dig.*, pp.313-316, 2009.
[3] International Technology Roadmap for Semiconductors, 2011 release.
[4] R. Kubo, J. Phys. Soc. Jpn. 12, 570 (1957).
[5] D. A. Greenwood, Proc. Phys. Soc. London 71, 585 (1958).
[6] R. Kotlyar *et al*, Appl. Phys. Lett. 84, 5270 (2004).
[7] E. B. Ramayya *et al*, IEEE Trans. NanoTechnol. 6, 113 (2007).
[8] S. Jin *et al*, J. Appl. Phys. 102, 083715 (2007).
[9] J.P. McKelvey *et al.*, *Physical Review,* vol. 123, no. 1, pp. 2736-2743, Jul. 1961.
[10] K. Natori, *J. Appl. Phys*., vol. 76, no. 8, pp. 4879-4890, Oct. 1994.
[11] M. Lundstrom *et al*, *IEEE Trans. Electron Devices*, vol. 49, no. 1, pp. 131-141, Jan. 2002.
[13] S. Martinie *et al*, *IEEE Elect. Device Lett*., vol. 29, no. 12, pp. 1392-1394, Dec. 2008.
[14] J. Dura *et al*, *IEEE Proc. SISPAD*, pp.43-46, 2011.
[15] S. Barraud, *J. Appl. Phys.*, vol.106, 063714, 2009.

(1)
$$\mu_{total}^{-1} = \left(\frac{\mu_{0,ph}}{E^{\theta_{ph}}}\right)^{-1} + \left(\frac{\mu_{0,SR}}{E^{\theta_{SR}}}\right)^{-1} + \left(\frac{\mu_{0,RCS}}{E^{\theta_{RCS}}}\right)^{-1}$$

with
$$\begin{cases} \mu_{0,ph}(D) = \mu_{bulk,ph} \cdot \sqrt{1 + A_{ph}.\delta D + B_{ph}.\delta D^4} \\ \mu_{0,SR}(D) = \mu_{bulk,SR} \cdot \left(1 + A_{SR}.\delta D + B_{SR}.\delta D^4\right)^6 \\ \mu_{0,RCS}(D) = \dfrac{\mu_{bulk,RCS}}{N_{fix}.\pi.\left(\frac{D}{2}\right)^2} \cdot \left(1 + A_{RCS}.\delta D + B_{RCS}.\delta D^4\right)^{3/2} \\ \delta D = \dfrac{D - D_{bulk}}{D_{bulk}} \end{cases}$$

D: nanowire diameter, *E*: electric field, μ_0: low-field mobility (*ph* phonon, *SR* surface roughness, *RCS* remote coulomb scattering), μ_{bulk}: bulk mobility, θ: electric field dependence, N_{fix}: trapped charge concentration in the gate oxide, *A/B*: fitting constant on Kubo-Greenwood results.

(2)
$$R = \frac{dfp^{-1}}{\frac{1}{2} L_{kT}^{-1} \cdot \left(1 + \coth\left(\frac{1}{2} \cdot \frac{L_c}{L_{kT}}\right)\right) + dfp^{-1}}$$

with
$$\begin{cases} L_{kT} = L_c \cdot \left(\dfrac{k.T}{q.V_{DS}}\right)^{1/\alpha} \\ \alpha = 1.9 + \left(\dfrac{dfp}{L_c}\right)^{0.7} \cdot \dfrac{1.7}{1 + e^{-\frac{L_c - 2D}{D}}} \\ dfp = \dfrac{2.k.T}{q.v_{inj}} \cdot \mu_{total} \end{cases}$$

V_{DS}: drain to source voltage, L_c: channel length, L_{kT}: kT-layer length, *dfp*: « dynamic free path », *k*: Boltzmann constant, *q*: electron charge, *T*: lattice temperature, v_{inj}: injection velocity.

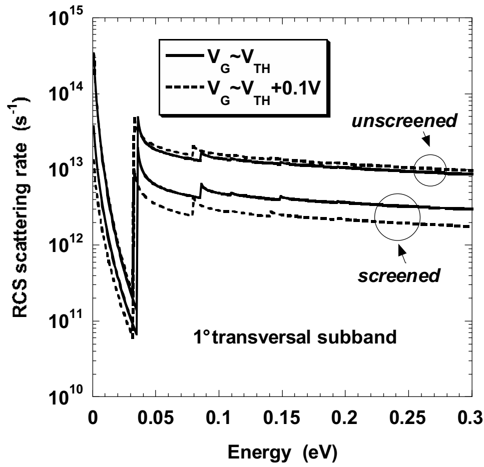

Fig. 1. RCS interaction frequency for the first transversal subband for two different polarizations (around threshold voltage V_{TH} and 0.1V higher). Comparison between the screened and unscreened cases.

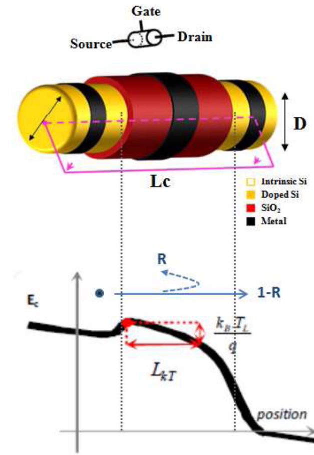

Fig. 3. Nanowire MOSFET schematics and energetic profile along the transport direction. Definition of the backscattering coefficient and the kT-layer.

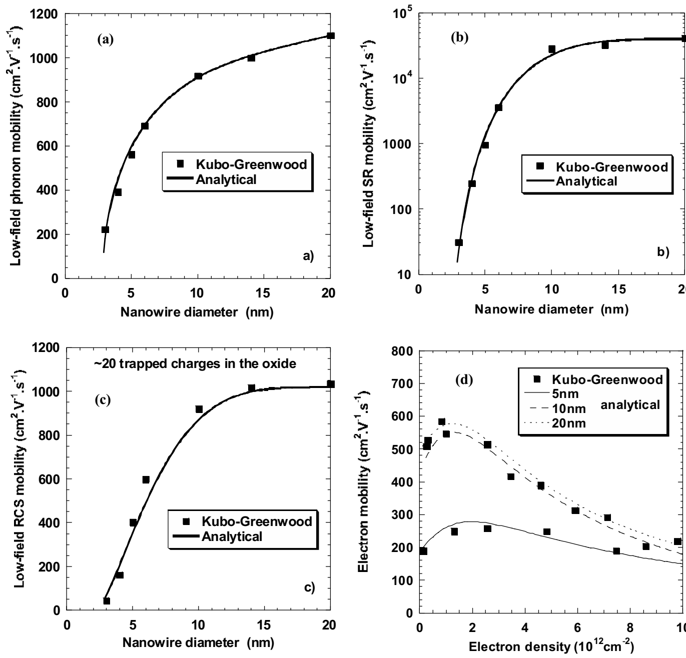

Fig. 2. Low-field mobilities for different scattering mechanisms (phonon (a), SR (b) and RCS (c)) with respect to the nanowire diameter. Then, electron mobility as a function of the electron density for different nanowire diameter (5, 10 and 20nm) (d). Comparison between analytical and Kubo-Greenwood model.

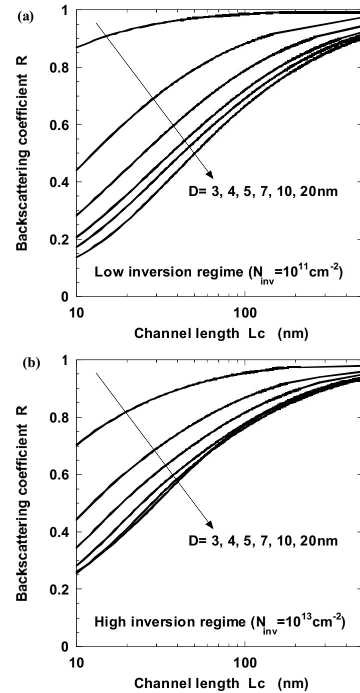

Fig. 4. Backscattering coefficient function of the channel length for different nanowire diameters (3, 4, 5, 7, 10 and 20nm) at low (a) and high (b) inversion regime.